Electronic Supplementary Material (ESI) for Journal of Materials Chemistry A.
This journal is © The Royal Society of Chemistry 2022

In-situ tailored strategy to remove capping agents from copper sulfide for building better lithium-sulfur batteries

Yuwei Zhao,[a, +] Donghai Wu,[b, +] Tingting Tang,[a, +] Chongguang Lyu,[a] Junfeng Li,[c] Shunping Ji,[c] Cheng-zong Yuan,[c] Kwan San Hui,[d] Chenyang Zha,[a,c,*] Kwun Nam Hui,[c,*] Houyang Chen,[e,*]

[a] Key Laboratory of Flexible Electronics (KLOFE), Institute of Advanced Materials (IAM), Nanjing Tech University, Nanjing 211816, Jiangsu, China

[b] Henan Key Laboratory of Nanocomposites and Applications, Institute of Nanostructured Functional Materials, Huanghe Science and Technology College, Zhengzhou 450006, Henan, China

[c] Institute of Applied Physics and Materials Engineering (IAPME), University of Macau, Taipa, Macau SAR, 999078, China

[d] Engineering, Faculty of Science, University of East Anglia, Norwich, NR4 7TJ, United Kingdom.

[e] Department of Chemical and Biological Engineering, State University of New York at Buffalo, Buffalo, NY 14260-4200, USA.

[+] These authors contributed equally to this article

[*] Corresponding authors:
iamcyzha@njtech.edu.cn (C. Zha)
chenyangzha@um.edu.mo (C. Zha)
bizhui@um.edu.mo (K.N. Hui)
hchen23@buffalo.edu (H. Chen)

Contents

Table S1..S3

Fig. S1...S4

Fig. S2...S5

Fig. S3...S6

Fig. S4...S7

Fig. S5...S8

Fig. S6...S9

Fig. S7...S10

Fig. S8...S11

Table S1. Electrochemical performances of Li-S batteries using C-$Cu_{1.93}S$ as cathode and previously reported Li-S batteries (all cells are charged at first).

Cathode catalyst	S loading [mg/cm^2]	Specific capacities [mAh/g]	Cycling stability [mAh/g]	Reference
C-$Cu_{1.93}S$	1.0	1207 at 0.8 mA/cm^2	580 after 500 cycles	**This work**
	2.0	1023 at 0.8 mA/cm^2	610 after 500 cycles	
TiS_2-NSC	2.5	1210 at 0.2 C	920 after 120 cycles	*Adv. Energy Mater.* 2019, 9, 1901872.
	2.5	1019 at 1 C	695 after 200 cycles	
TiS_2-NSC-CFs	5.3	1045 at 0.1 C	734 after 200 cycles	
	7.7	1025 at 0.1 C	767 after 100 cycles	
NiS-C-HS	1.0	1002 at 0.2 C	718 after 200 cycles	*Adv. Funct. Mater.* 2017, 27, 1702524.
	2.3	723 at 0.5 C	695 after 300 cycles	
ZnS-FeS/NC	2.01	Not given at 0.2 C	823 after 200 cycles	*J. Mater. Chem. A,* 2020, 8,433.
	2.40	Not given at 0.2 C	811 after 200 cycles	
	3.34	Not given at 0.2 C	796 after 200 cycles	
VS-NT	6.4	944.9 at 0.2 C	661 after 200 cycles	*ACS Energy Lett.* 2019, 4, 755-762.
	9.6	1356 at 0.1 C	952 after 120 cycles	
SnS_2-ND/G	2.5	1234 at 0.2 C	1016 after 300 cycles	*J. Mater. Chem. A*, 2018, *6*, 7659.
ZnS-CB	1.37	876 at 2 C	632 after 1000 cycles	*Nano Energy*, 2018, 51, 73.
	1.37	657 at 5 C	388 after 1000 cycles	
G-VS_2	1.0	1270 at 1 C	923 after 150 cycles	*Adv. Energy Mater.*, 2018, 1800201.
	2.0	786 at 1 C	559 after 150 cycles	
	3.5	701 at 1 C	520 after 150 cycles	
G-Cu_2S-S-C	3.5	953 at 0.5 C	720 after 300 cycles	*J. Mater. Chem. A*, 2019, *7*, 12815.
		809 at 1 C	580 after 800 cycles	
		635 at 2 C	441 after 800 cycles	

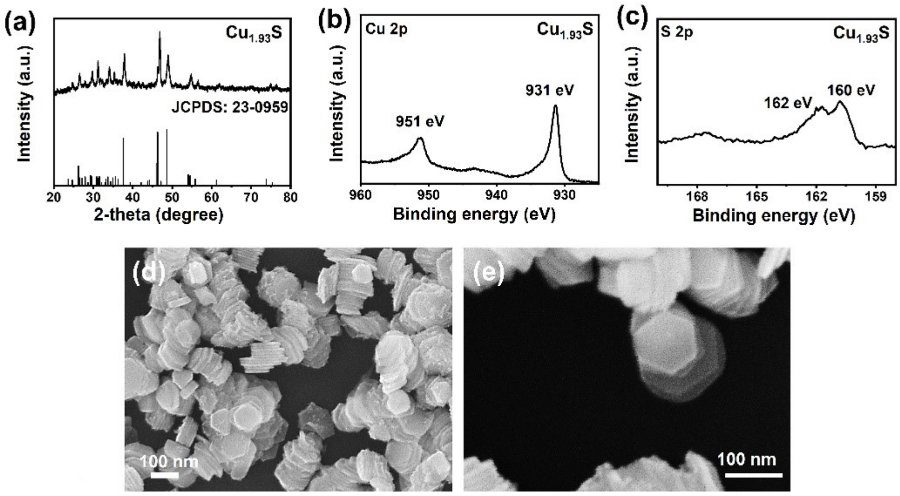

Fig. S1. Structural characterizations of $Cu_{1.93}S$. The XRD pattern (a), XPS spectra of Cu 2p (b) and S 2p (c), SEM images (d-e).

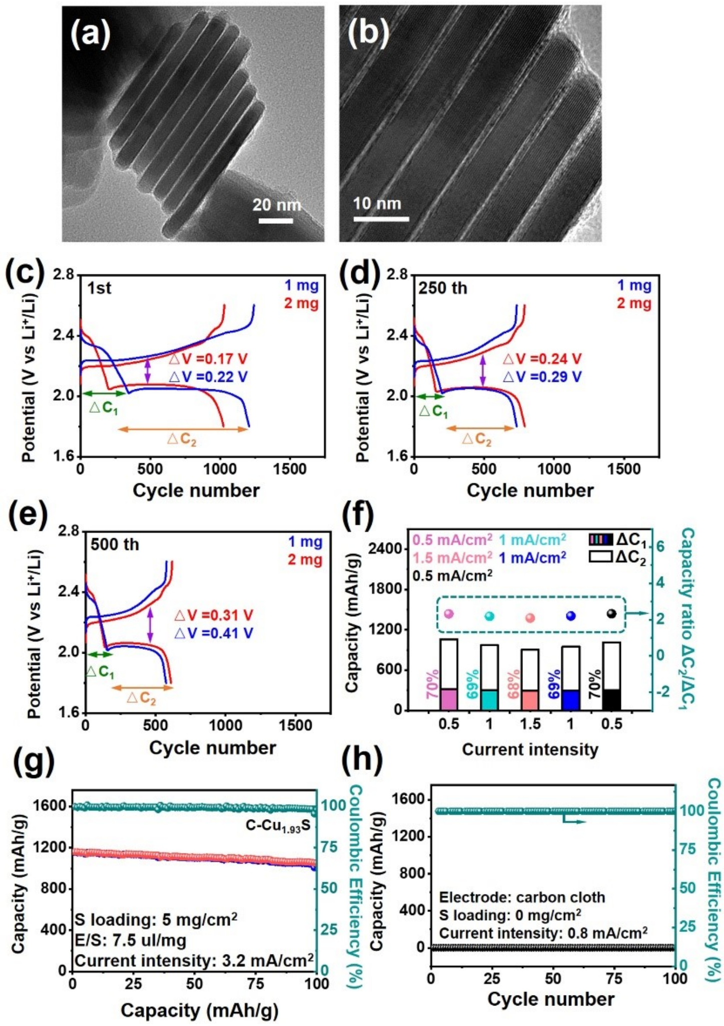

Fig. S2. TEM images (a-b) of C-$Cu_{1.93}S$. The charge and discharge profiles at 1st (c), 250th (d) and 500th (e) of C-$Cu_{1.93}S$-based Li-S cells under different sulfur loading. The C-$Cu_{1.93}S$-based Li-S cell with capacity ratios image (f) of $\Delta C_2/\Delta C_1$ under different current. The cycling stability and Coulombic efficiency (g) of C-$Cu_{1.93}S$-based Li-S cells. The cycling stability and Coulombic efficiency (h) of pure carbon cloth-based cells.

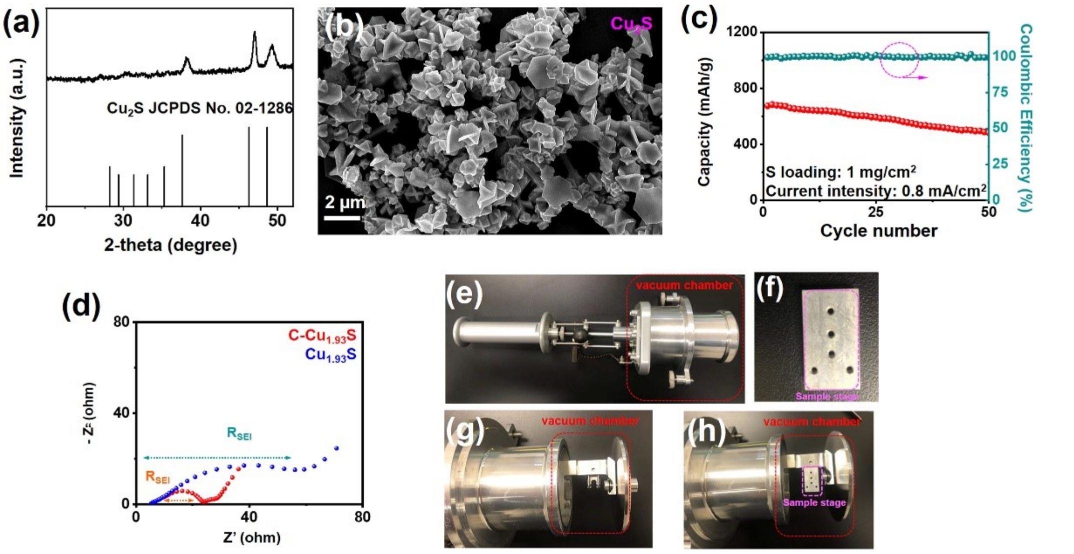

Fig. S3. XRD pattern (a), SEM image (b) of Cu_2S materials, and cycling performance of Cu_2S-based cell (c). The EIS of C-$Cu_{1.93}S$ and $Cu_{1.93}S$-based symmetric cells (d). Optical photographs (e-h) of in-situ technology-based chamber of XPS.

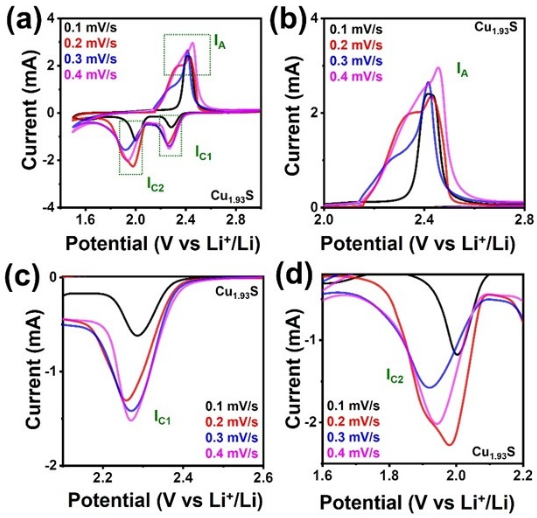

Fig. S4. Rated CV curves from 0.1 to 0.4 mV/s (a) with the corresponding magnified redox peaks (b-d).

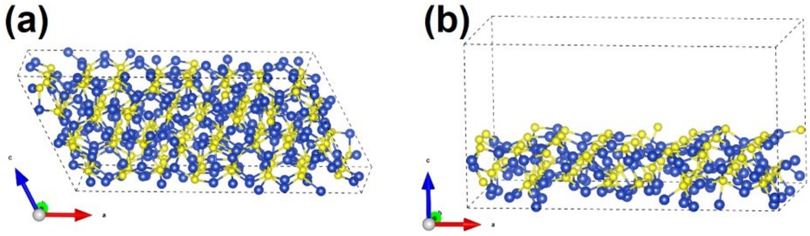

Fig. S5. Crystal structure of C-$Cu_{1.93}S$.

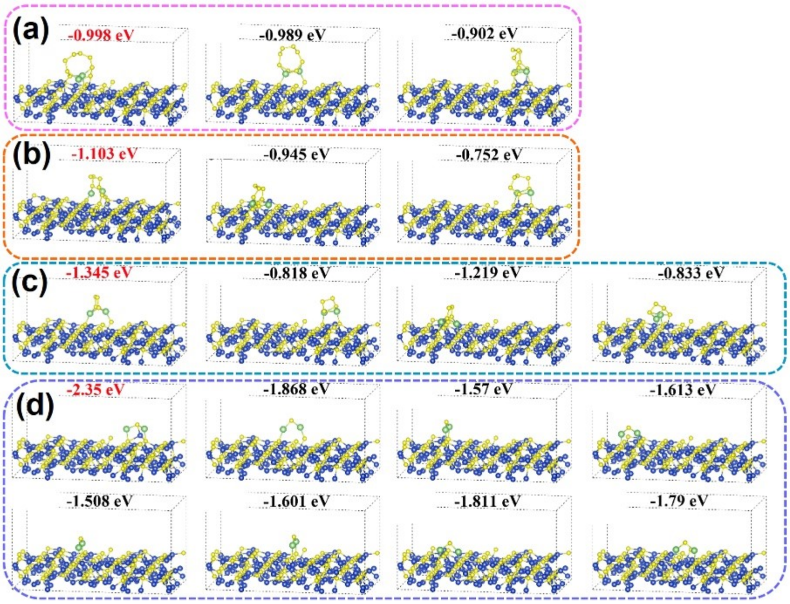

Fig. S6. Several possible configurations of Li_2S_8 (a), Li_2S_6 (b), Li_2S_4 (c) and Li_2S (d) adsorption on the $Cu_{1.93}S$ (004) surface.

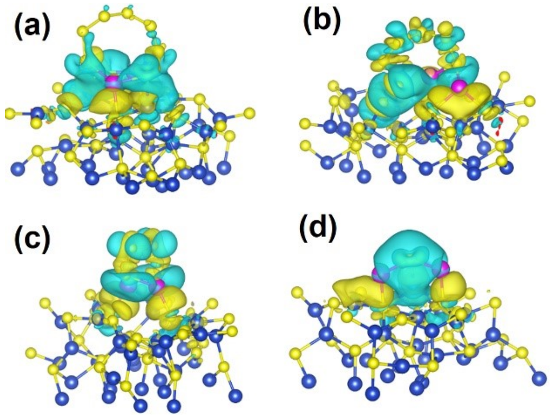

Fig. S7. The charge density difference of the energy most favorable configurations for Li_2S_8 (a), Li_2S_6 (b), Li_2S_4 (c), and Li_2S (d) adsorption on $Cu_{1.93}S$ (004) surface. Cyan and yellow regions represent the charge depletion and accumulation in space, respectively.

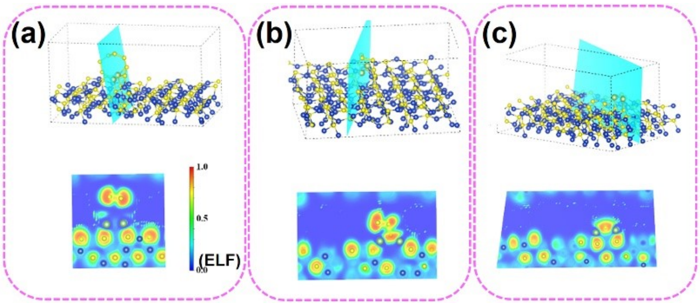

Fig. S8. The electron local function plots of the energy most favorable configurations of a pure $Cu_{1.93}S$ (004) surface with the adsorption of Li_2S_8 (a), Li_2S_6 (b), and Li_2S (c).